Supplementary Materials (Taghi Khani *et al*.)

Isoform-specific knockdown of long and intermediate prolactin receptors interferes with evolution of B-cell neoplasms

Inventory

- Supplementary Figures S1-S11
- Supplementary Tables S1 and S2

Figure S1: *Gating strategy for flow cytometry analysis of mouse splenic WBCs.*

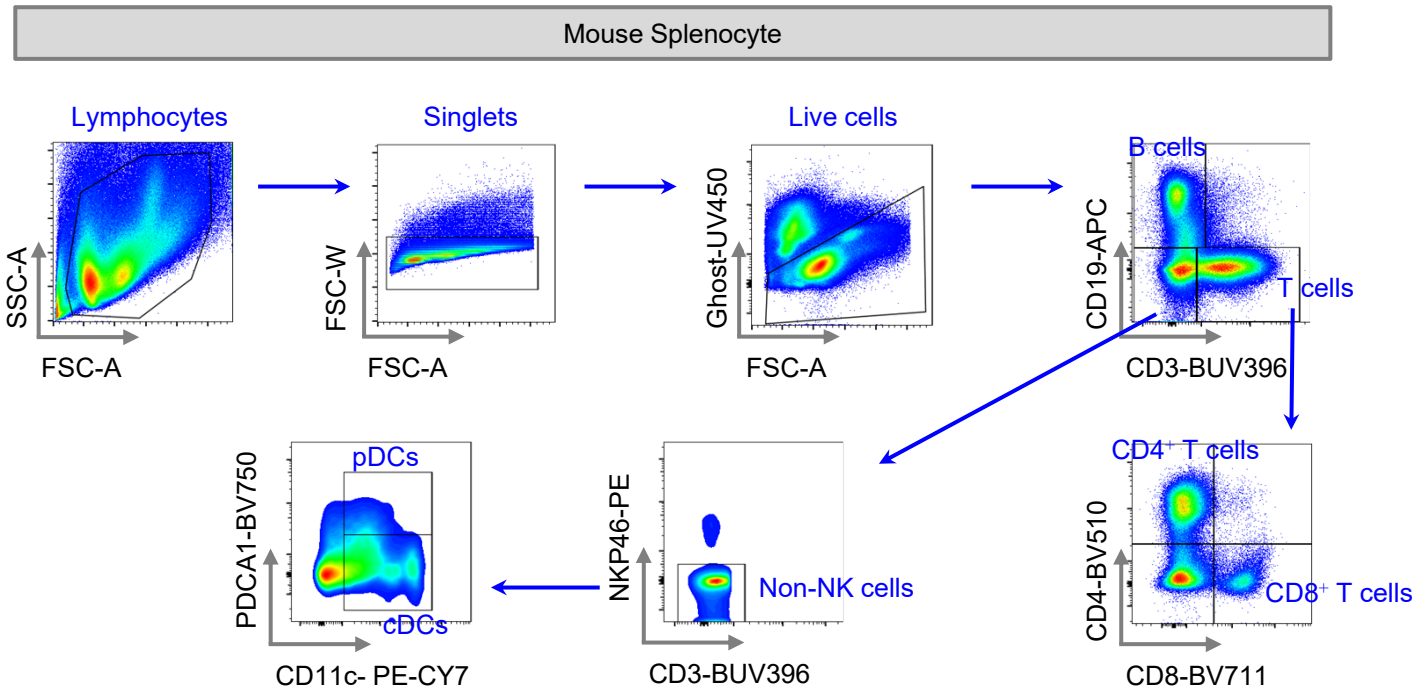

Figure S1: Gating strategy for flow cytometry analysis of mouse splenic WBCs. From the lymphocyte cluster; singlets were gated followed by selection of live (Ghost-UV450^{-}) populations. B cells, T cells, and non-B non-T cells were then gated on CD19^{+}, CD3^{+}, and CD19^{-} CD3^{-}, respectively. T cells were gated on CD8^{+}, CD4^{+}, and CD4^{-}CD8^{-} T cells. pDCs and cDCs were gated on CD11c and PDCA1 after gating out NKp46^{+} NK cells from the non-B non-T fraction.

Figure S2: *LFPRLR knockdown did not induce significant changes in numbers of T cell subsets in SLE prone mice.*

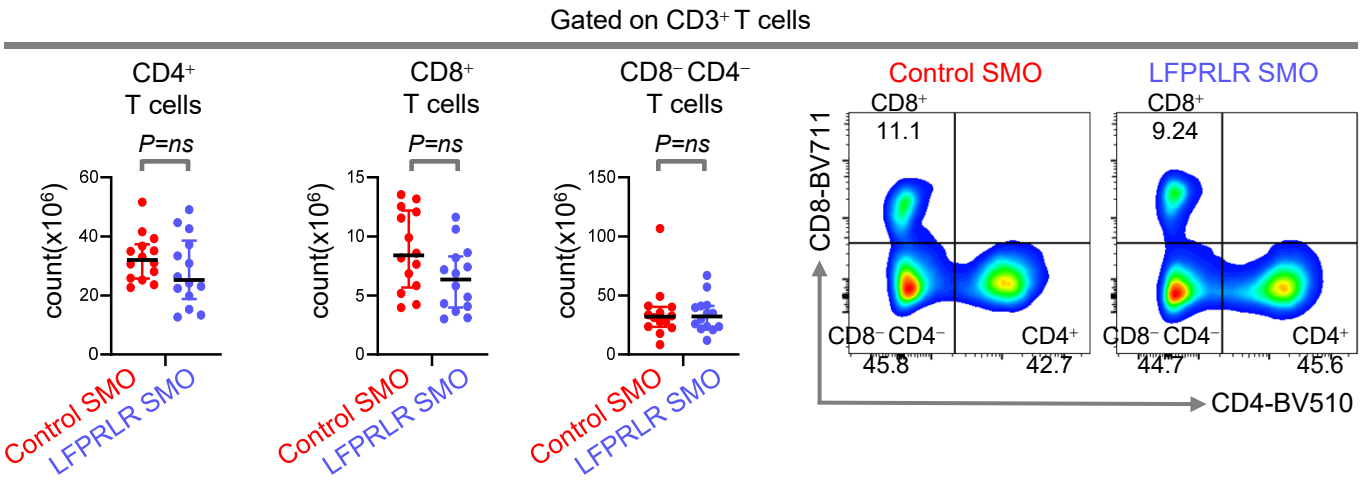

Figure S2: LFPRLR knockdown did not induce significant changes in frequencies or numbers of T cell subsets in SLE-prone mice. Quantitation of numbers and representative flow cytometry plots of $CD4^+$, $CD8^+$, and $CD4^-CD8^-$ T cells of *MRL-lpr* SLE prone mice treated with control SMO (n=14, red) or LFPRLR SMO to knockdown LFPRLR (n=14, blue). Graphs show median ± interquartile range. Exact p-values were calculated using the Mann-Whitney U test. ns = non-significant.

Figure S3: *Gating strategy for flow cytometry by intracellular staining.*

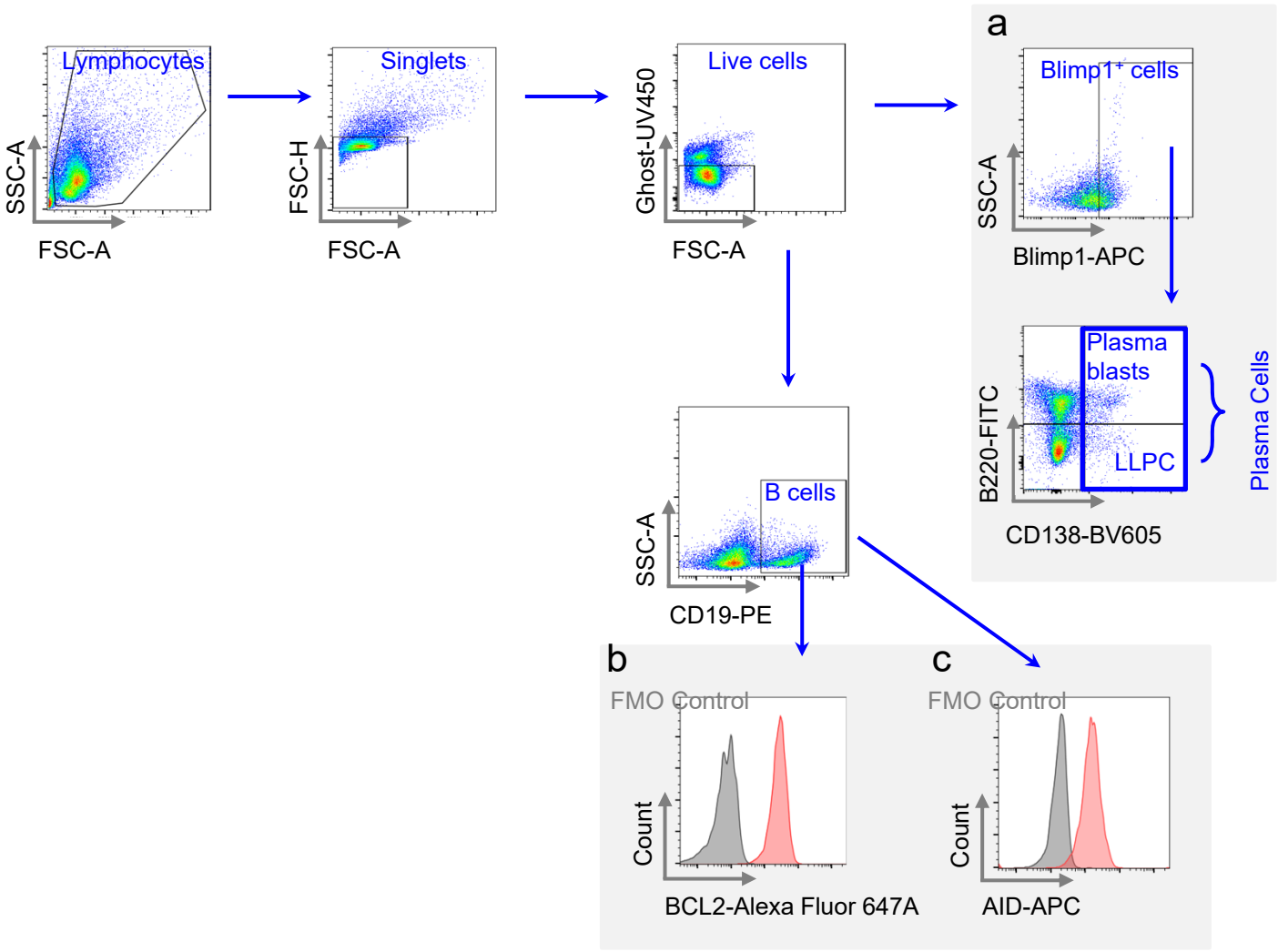

Figure S3: Gating strategy for flow cytometry by intracellular staining. From the lymphocyte cluster; singlets were gated followed by selection of live (Ghost-UV450^{-}) populations. (**a**)Total CD138^{+} plasma cells, CD138^{+}B220^{+} plasmablasts, and CD138^{+}B220^{-} LLPC were then measured by gating on Blimp1^{+}cells. (**b-c**) Total CD19^{+} B cells were then gated and BCL2 **(b)** or AID **(c)** was measured within these cells. Gates for all markers were set based on fluorescence minus one controls (FMO).

Figure S4: *Gating strategy for flow cytometry analysis and magnetic sorting of mouse splenic B cells*

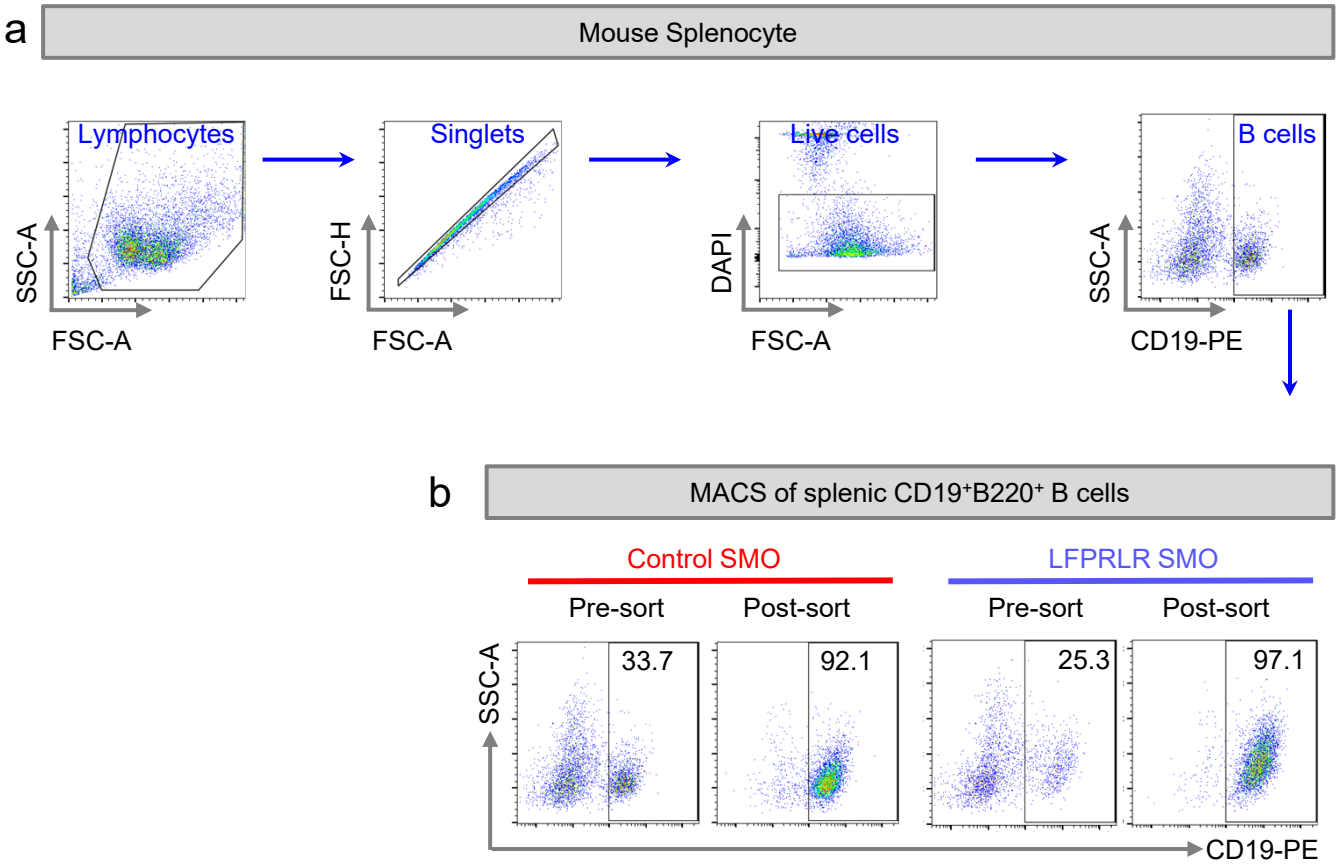

Figure S4: Gating strategy for flow cytometry analysis and magnetic sorting of mouse splenic B cells. (a) From the lymphocyte cluster; singlets were gated followed by selection of live (Ghost-UV450^{-}) populations. B cells were then gated on CD19^{+}. **(b)** Flow cytometry verification of splenic B cells sorted out magnetically using CD19 microbeads from one representative 14-week-old *MRL-lpr* SLE-prone mouse treated with either control SMO (n=14) or LFPRLR SMO (n=14) for 8 weeks.

Figure S5: *LFPRLR knockdown did not induce significant changes in numbers of T cell and DC subsets in DLBCL prone mice.*

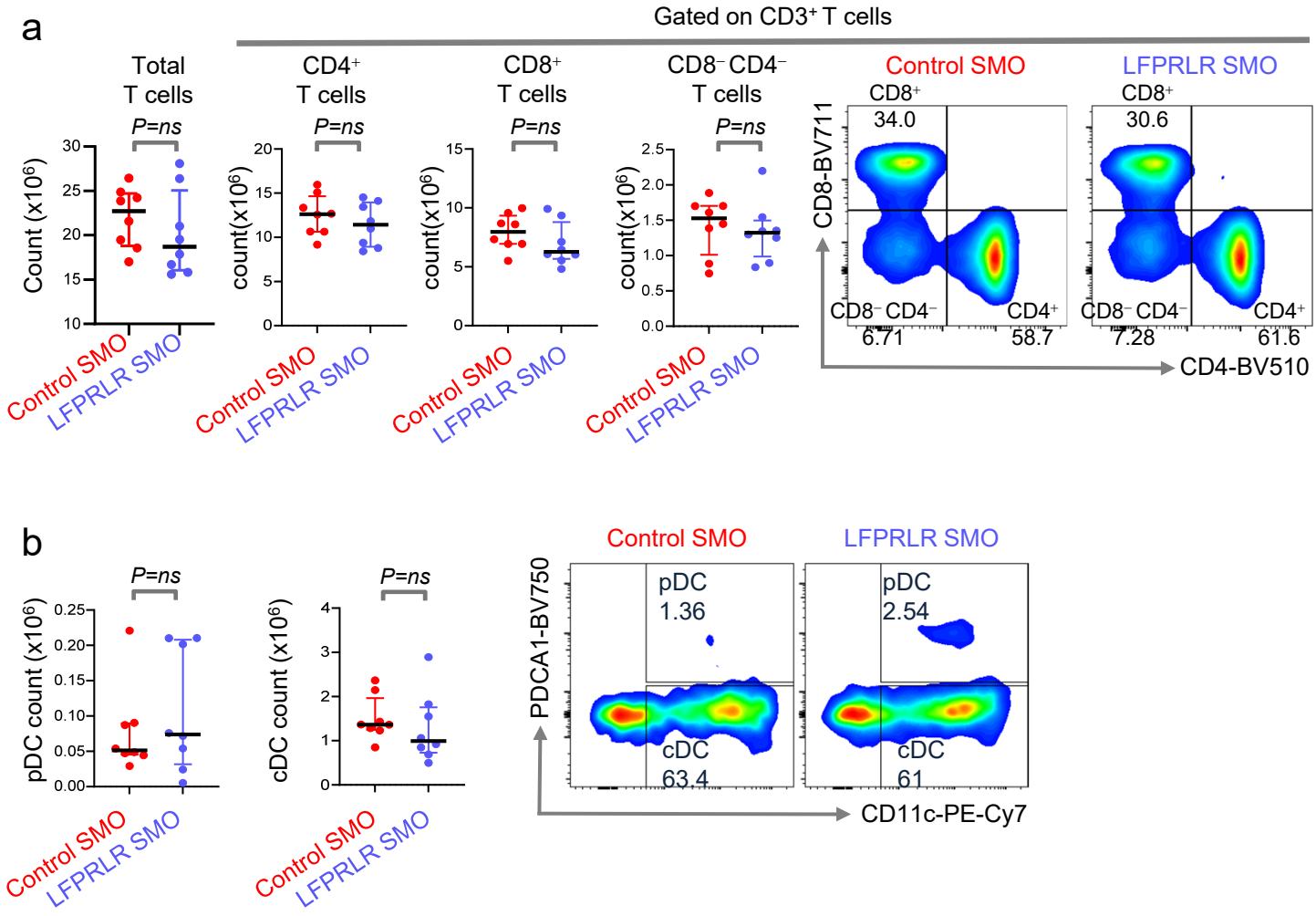

Figure S5: LFPRLR knockdown did not induce significant changes in numbers of T cell and DC subsets in DLBCL-prone mice. (a,b) Quantitation of numbers and representative flow cytometry plots of total, $CD4^+$, $CD8^+$, and $CD4^-CD8^-$ T cells (**a**) and $CD11c^+PDCA1^+$ pDCs and $CD11c^+PDCA1^-$ cDCs (**b**) in *TCL1*-tg DLBCL-prone mice treated with control SMO (n=8, red) or LFPRLR SMO to knockdown LFPRLR (n=8, blue). Graphs show median ± interquartile range. Exact p-values were calculated using the Mann-Whitney U test. ns = non-significant.

Figure S6: *Knockdown of LFPRLR in DLBCL-prone mice does impact cycling of splenic B cells*

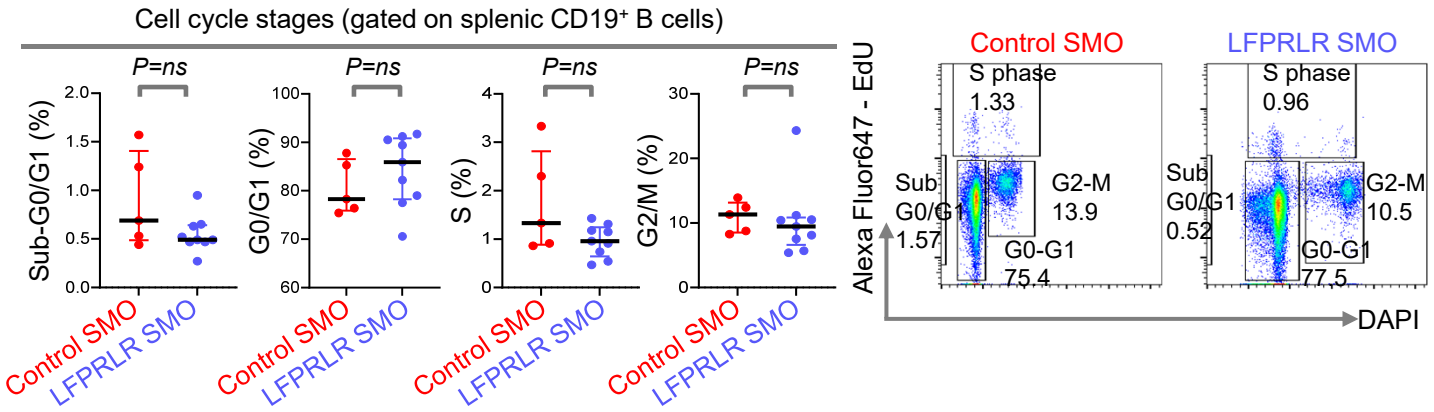

Figure S6: Knockdown of LFPRLR in DLBCL-prone mice does not impact cycling of splenic B cells. Percentages of B cells in sub G0/G1, G0/G1, S, G2/M phases and representative flow cytometry in spleens of *TCL1-tg* mice treated with control SMO (n=8, red) or LFPRLR SMO (n=8, blue). Graphs show median ± interquartile range. Exact p-values were calculated using the Mann-Whitney U test. ns = non-significant.

Figure S7: *Knockdown of LFPRLR reduced BCL2 expression but does not alter MYC expression in total splenic WBCs of DLBCL-prone mice*

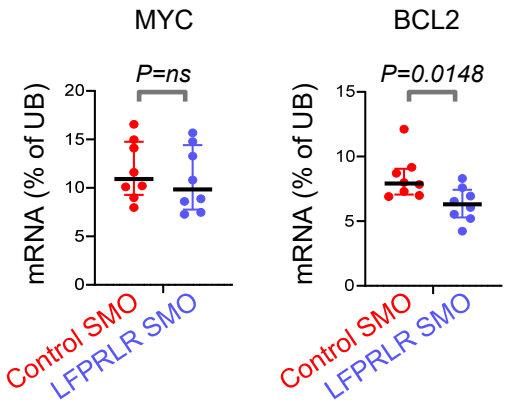

Figure S7: Knockdown of LFPRLR reduced BCL2 expression but does not alter MYC expression in total splenic WBCs of DLBCL-prone mice. Comparison of total splenocyte transcript levels of MYC (*left*) and BCL2 (*right*) by qPCR in *TCL1-tg* mice treated with control SMO (n=8, red) or LFPRLR SMO (n=8, blue). Graphs show median ± interquartile range. Each dot in qPCR analyses of transcripts corresponds to the mean expression of that gene in one mouse calculated from 3 technical replicates. Exact p-values were calculated using the Mann-Whitney U test. ns = non-significant

Figure S8: *Total PRLR expression in diagnosis and treated DLBCL patients does not predict clinical outcome*

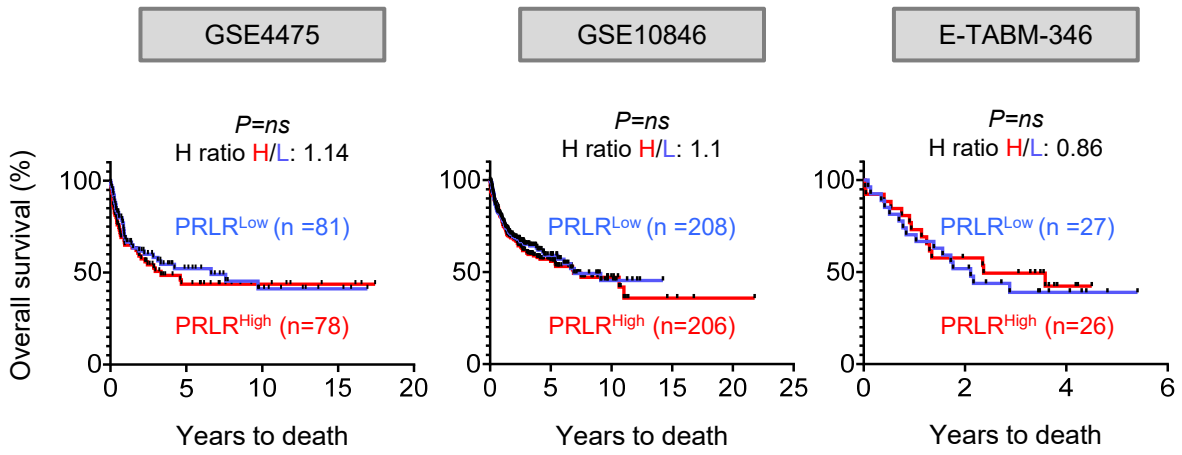

Figure S8: Total PRLR expression in diagnosis and treated DLBCL patients does not predict clinical outcome. Comparison of overall survival probabilities of patients with B cell lymphomas from 3 datasets (GSE4475, GSE10846, and E-TABM-346) divided into two groups as $PRLR^{High}$ and $PRLR^{Low}$ based on the median expression of total PRLR mRNA. GSE4475 includes 123 DLBCL and 36 BL patients at diagnosis. GSE10846 includes samples from 414 DLBCL patients collected after treatment with Rituximab-CHOP or CHOP and E-TABM-346 includes samples from 53 DLBCL patients collected after treatment with Rituximab-CHOP or CHOP. P values were measured by Log-rank (Mantel-Cox) test. ns=not significant

Figure S9: *Normal B cells always express both SFPRLR and LF/IF PRLR but 50% of BCL2/MYC-driven B-ALL express only LF/IF PRLR*

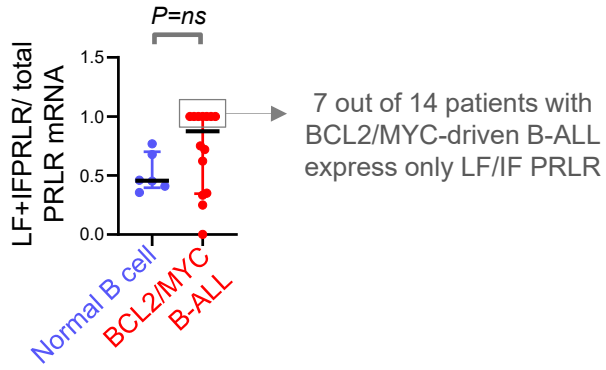

Figure S9: Normal B cells always express both SFPRLR and LF/IF PRLR but 50% of BCL2/MYC-driven B-ALL express only LF/IF PRLR. Comparison of expression of ratio of LF+IF: total PRLR between normal B cells and patients with BCL2/MYC-driven B-ALL from the St. Jude cohort EGAS00001003266. Graph shows median ± interquartile range. Exact p-value was calculated using the Mann-Whitney U test. ns = non-significant.

Figure S10: *Gating strategy for flow cytometry analysis and magnetic sorting of human peripheral blood B ,T and NK cells*

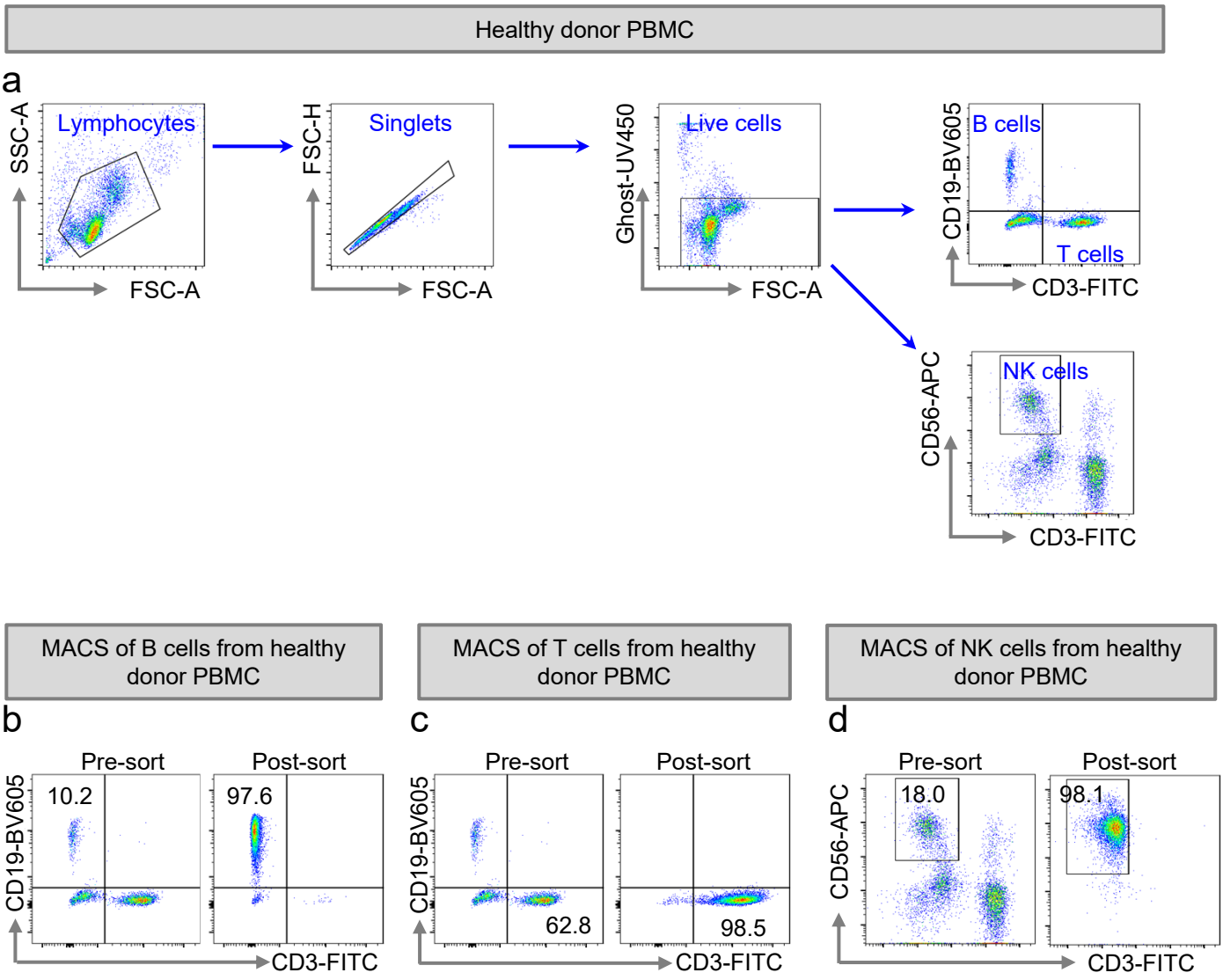

Figure S10: Gating strategy for flow cytometry analysis and magnetic sorting of human peripheral blood B, T and NK cells. (a) From the lymphocyte cluster; singlets were gated followed by selection of live (Ghost-UV450^{-}) populations. B cells were then gated on CD3^{-} CD19^{+}, T cells were gated on CD3^{+} CD19^{-} and NK cells were then gated on CD3^{-}CD56^{+}. **(b-d)** Verification of post-sort purity of magnetically sorted B (b), T (c) and NK (d) cells from PBMC of healthy donors by flow cytometry.

Figure S11: *Full scan of blot shown in Figure 5c,d*

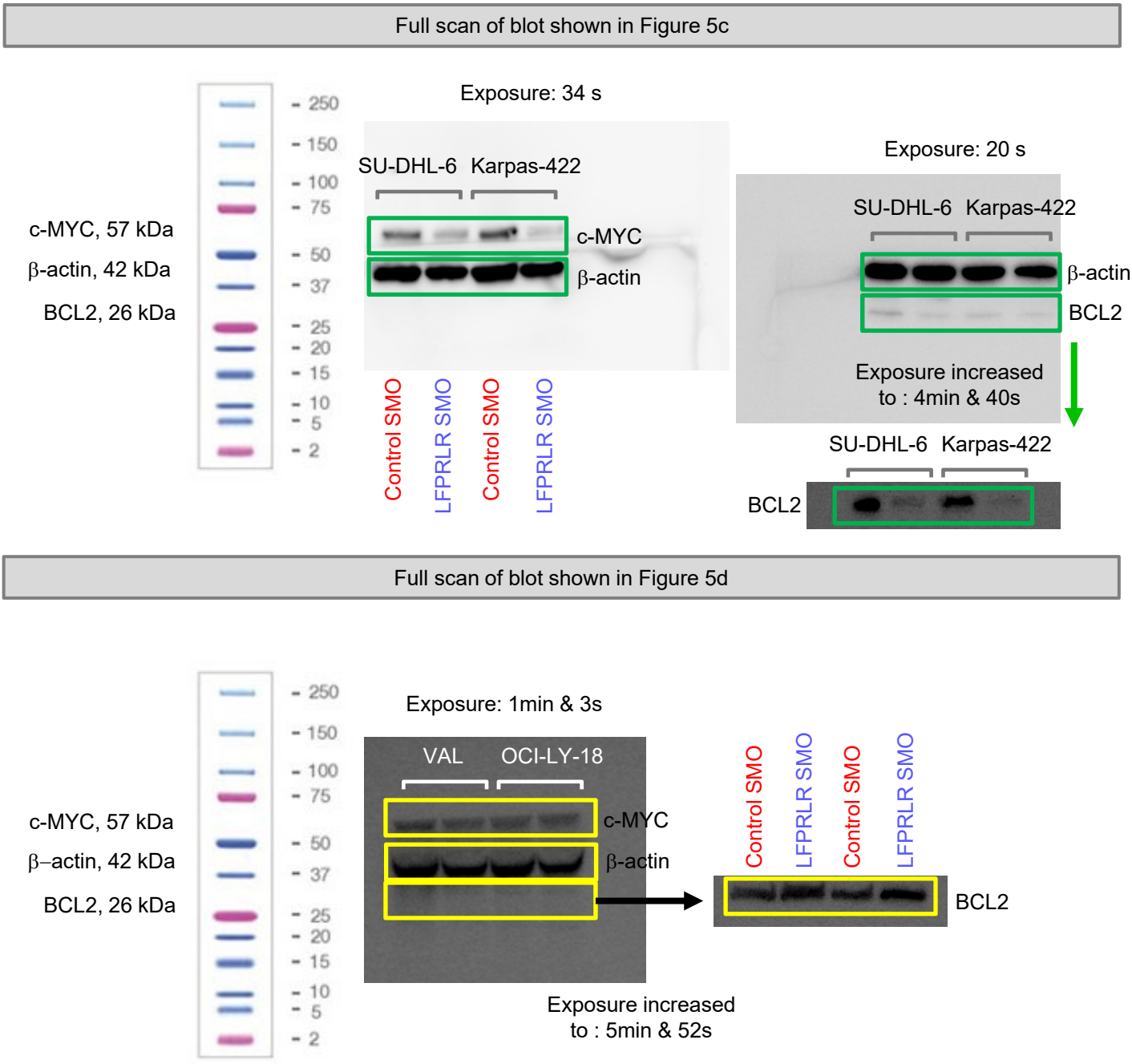

Figure S11: Full scan of blot shown in Figure 5c,d. Blot was developed in ChemiDoc MP imaging system (BioRad)

Table S1: *List of oligonucleotide sequences used in the study*

a. Splice modulating oligomer

SMO	Sequence
Control SMO	5'-AGACGAGATTCGATCGGAGTA-3'
mLFPRLR SMO	5'-GCCCTTCTATTGAAACACAGATACA-3'
hLFPRLR SMO	5'-GCCCTTCTATTAAAACACAGACACA-3'

b. Quantitative RT-PCR

Primer	Sequence
mUB- F	5'-AGCCCAGTGTTACCACCAAG-3'
mUB- R	5'-ACCCAAGAACAAGCACAAGG-3'
mLFPRLR- F	5'-ATAAAAGGATTTGATACTCATCTGCTAGAG-3'
mLFPRLR- R	5'-TGTCATCCACTTCCAAGAACTCC-3'
mSF1PRLR- F	5'-AAGCCAGACCATGGATACTGGAG-3'
mSF1PRLR- R	5'-AACTGGAGAATAGAACACCAGAG-3'
mSF2PRLR- F	5'-TGCATCTTTCCACCAGTTCCGGGGC-3'
mSF2PRLR- R	5'-TCAAGTTGCTCTTTGTTGTCAAC-3'
mSF3PRLR- F	5'-TGCATCTTTCCACCAGTTCCGGGGC-3'
mSF3PRLR- R	5'-TTGTATTTGCTTGGAGAGCCAGT-3'
mMYC- F	5'-TCGCTGCTGTCCTCCGAGTCC-3'
mMYC- R	5'-GGTTTGCCTCTTCTCCACAGAC-3'
mBCL2- F	5'-CCTGTGGATGACTGAGTACCTG-3'
mBCL2- R	5'-AGCCAGGAGAAATCAAACAGAGG-3'
mAID- F	5'-AAATGTCCGCTGGGCCAA-3'
mAID- R	5'-CATCGACTTCGTACAAGGG-3'
hUB- F	5'-GCCGCACTCTTTCTGACTACAAC-3'
hUB- R	5'-ACCTCCAGAGTGATGGTCTTGC-3'
hLF/IFPRLR- F	5'-TCCAGGTATGTGGGTTTCAT-3'
hLF/IFPRLR- R	5'-GATTTGATGCTCATCTGTTGGA-3'
hSF1aPRLR- F	5'-TGGACTGTGGTCAATGTTGC-3'
hSF1aPRLR- R	5'-GATAGTGAGGACCAGCATCTAATG-3'
hSF1bPRLR- F	5'-CAACATCAAGGGGTCACCTC-3'
hSF1bPRLR- R	5'-CATGAATGATACAACCGTGTGG-3'
hMYC- F	5'-CCTGGTGCTCCATGAGGAGAC-3'
hMYC- R	5'-CAGACTCTGACCTTTTGCCAGG-3'
hPRL- F	5'-GAGGAGCAAACCAAACGGCTTC-3'
hPRL- R	5'-AAGGCGAGACTCTTCATCAGCC-3'
hBCL2- F	5'-ATCGCCCTGTGGATGACTGAGT-3'
hBCL2- R	5'-GCCAGGAGAAATCAAACAGAGGC-3'

c. *mIGH* sequencing

Primer	Sequence
V_H1_F	5'-AAGGCCACACTGACTGTAGAC-3'
Cμ_R	5'-TGGCCACCAGATTCTTATCAG-3'

Table S2: *List of antibodies used in the study*

a. Flow cytometry

Antibodies	Clone ID	Specificity	Dilution	Source
Anti-CD19	1D3/CD19	Mouse	7:1000	Biolegend
Anti-CD45R/B220	RA3-6B2	Mouse/Human	5:1000	Biolegend
Anti-CD138 (Syndecan-1)	281-2	Mouse	1:100	Biolegend
Anti-Blimp-1	5E7	Mouse	1:100	Biolegend
Anti-AID	mAID-2	Mouse/Human	1:100	eBioscience
Anti-BCL2	BCL/10C4	Mouse/Rat	1:100	Biolegend
Anti-CD3	UCHT1	Human	1:100	Biolegend
Anti-CD56	5.1H11	Human	1:100	Biolegend
Anti-CD19	HIB19	Human	1:100	Biolegend
Anti-CD4	RM4-5	Mouse	1:100	Biolegend
Anti-CD19	1D3	Mouse	1:100	BD
Anti-CD11c	N418	Mouse	1:100	Biolegend
Anti-CD8	5306.7	Mouse	1:100	Biolegend
Anti-CD3	17A2	Mouse	1:100	BD
Anti-PDCA1	927	Mouse	1:100	BD
Anti-NKP46	29A1.4	Mouse	1:100	BD
Ghost Dye™ UV 450			1:100	Tonbo

b. Immunoblotting

Antibodies	Clone ID	Specificity	Dilution	Source
Anti-cMYC	D84C12	Mouse/Human	1:1000	Cell Signaling Technology
Anti-β-Actin	8H10D10	Mouse/Human	1:500	Cell Signaling Technology
Anti-BCL2	D17C4	Mouse/Human	1:1000	Cell Signaling Technology